PERGAMON

International Journal of Multiphase Flow 26 (2000) 1831–1850

International Journal of Multiphase Flow

www.elsevier.com/locate/ijmulflow

Particles-turbulence interaction in stationary, homogeneous, isotropic turbulence

G. Ooms*, G.H. Jansen

J.M. Burgerscentrum, Laboratory for Aero- and Hydrodynamics, Technological University Delft, Rotterdamseweg 145, 2628 AL, Delft, The Netherlands

Received 7 October 1998; received in revised form 1 December 1999

Abstract

A physical model for the dynamics of a dispersion of solid spherical particles in an incompressible viscous fluid is outlined and used to calculate the turbulence modulation in a stationary, homogeneous and isotropic turbulent flow with particles. Starting from a postulated fluid turbulence spectrum in the absence of particles, the physical model predicts the corresponding fluid turbulence spectrum in the presence of particles and the particles turbulence spectrum as function of frequency and wavenumber. There are two versions of the model. The first one uses a point-force approximation for the particles and takes into account the hydrodynamic interaction between the particles. The second version accounts for the detailed flow around the (finite-diameter) particles, but does not consider their hydrodynamic interaction. The spectra, calculated with the two versions, are used to determine the turbulence intensity of the fluid and particles as function of three relevant dimensionless groups. It is found that in general the differences between the results of the point-particle model and the finite-diameter-particle model are significant. So one has to be careful with point-particle models. The effect of the hydrodynamic interaction between the particles is up to a volume fraction of 0.1 still mostly negligible.

Keywords: Particles; Two-phase flow; Particle-turbulence interaction; Turbulent fluctuations

1. Introduction

Turbulent fluid-particles flows are encountered in a wide variety of applications. An accurate

* Corresponding author.

PII: S0301-9322(99)00121-4

computation method for such flows is essential, in order to be able to interpret and predict experimental data and to support the scaling-up of applications. For that reason much interest has been devoted to turbulent fluid-particles flows and in particular to the possibility of modeling them. See, for instance, the recent book by Crowe et al. (1998).

An important issue in the development of calculation methods for turbulent fluid-particles flows is the influence of the particles on the turbulence of the carrier phase. In particular, in the review article by Crowe et al. (1996), much information is given about the literature on this two-way coupling effect. Gore and Crowe (1989) gathered data from a variety of researchers in order to generalize a trend for turbulence attenuation or augmentation and found that the ratio of particle diameter to integral length scale of the fluid turbulence is important. Squires and Eaton (1990) investigated the modification of turbulence by small particles using direct numerical simulations of stationary, isotropic turbulence. Examination of the spatial energy spectra showed that the fraction of turbulence kinetic energy in the high wave numbers is increased relative to the energy in the low wave numbers for increasing values of the particle mass loading. Elgobashi and Truesdell (1993), using direct numerical simulations, studied the modification of decaying, homogeneous turbulence due to its interaction with dispersed small solid particles. They also paid particular attention to the modification of the turbulence spectra. Portela et al. (1998) used large-eddy simulation to investigate a channel flow laden with small heavy particles. Their main result concerning the two-way coupling was that it dampens the fluid velocity fluctuations and reduces the concentration of particles near the wall. Elgobashi and Abou-Arab (1983) developed a two-equation turbulence model for predicting two-phase flows (describing fluid and particles as a continuum). The two equations describe the conservation of turbulence kinetic energy and dissipation rate of that energy for the carrier fluid. Closure is achieved by modeling the turbulence correlations up to third order. Lun and Liu (1997) applied a two-equation turbulence model too. However, the solid phase is simulated by using a Lagrangian approach, in which the particles trajectories and velocities are determined by integrating the particle equation of motion.

Also several physical models have been proposed for the turbulence modification by particles. For instance, Yarin and Hetsroni (1994) proposed a model for the particles-turbulence interaction, in which both turbulence suppression by the fine particles and turbulence enhancement by the coarse particles are considered. They found that the intensity of the velocity fluctuations is determined by four parameters: the total mass content of the fluid–particles mixture, the fluid–particle density ratio, the particle Reynolds number, and the ratio of the particle size and turbulence length scale. The results of their study are in fair agreement with experiments. Yuan and Michaelides (1992) presented also a model for the turbulence modification in particle-laden flows based on the interaction between particles and turbulence eddies. Two predominant mechanisms for the suppression and production of turbulence were identified: (1) the acceleration of particles in eddies is the predominant mechanism for turbulence reduction, and (2) the flow velocity disturbance due to the wake of particles or the vortices shed by the particles is taken to be the predominant mechanism for turbulence enhancement. The effect of the two mechanisms were combined to yield the overall turbulence intensity modification. The model exemplifies the effect of several variables, such as particle size, relative velocity, Reynolds number, ratio of densities, etc. Again a comparison with available experimental data confirmed that this model predicts rather well the observed changes

in turbulence intensity. Finally, Kenning and Crowe (1997) developed a model for carrier phase turbulence in gas–particles flows. The model suggests the importance of interparticle spacing in establishing a turbulence length scale in particles–gas suspensions.

A different type of physical model to investigate the turbulence modification by particles has been developed by Felderhof and Ooms (1989, 1990), further extended by Felderhof and Jansen (1991). They developed a model for the dynamics of a dispersion of solid spherical particles in an incompressible viscous fluid, in particular, paying attention to the influence of the particle–fluid interaction on the effective transport coefficients of the fluid–particles suspension. The calculations of Felderhof and Ooms were based on a point-force approximation (in which a force field exerted by a particle on the fluid is represented by a point force acting on the fluid at the particle center) with a friction coefficient given by Stokes' law. The work by Felderhof and Jansen takes the full force field exerted by the finite-diameter particle on the fluid into account. The study by Felderhof and Jansen ignores the hydrodynamic interaction between the particles, unlike the model of Felderhof and Ooms. The calculation scheme based on Felderhof and Jansen's study can handle the hydrodynamic interaction between the particles in principle, but the calculations are very tedious and computationally intensive.

The aim of this publication is to use the two versions of the physical model developed by Felderhof and Ooms and by Felderhof and Jansen, to calculate the influence of the particles on the turbulence intensity of the fluid as function of the relevant parameters. The turbulence is assumed to be stationary, homogeneous and isotropic. By comparing the results of the two versions the reliability of the point-particle approximation can be studied. Also the importance of including the hydrodynamic interaction between the particles can be investigated. The results will, of course, also be compared with results of publications discussed above. Next to an improved fundamental understanding, another aim of our work is to contribute to the development of better two-fluid models. At the moment it is not clear, how it can be achieved. A possibility is to use our model to check and (if necessary) improve the source term in the turbulent energy equation of two-equation turbulence models for two-phase flows. We are investigating this at the moment. Another possibility could be to calculate with our model the turbulence energy and dissipation (the dissipation can be calculated from the energy spectra) in each part of the flow domain, and to use the energy and dissipation directly for closure of the correlation terms in the mean momentum equations.

This publication is organized as follows. In Section 2 and Appendices A and B, the physical model is discussed. Section 3 gives the calculation method for the turbulence intensities of the fluid and particles. In Section 4, the numerical results for these intensities are summarized, a comparison is made with the results of other studies and conclusions are drawn. We conclude in Section 5 with suggestions for future research.

2. Physical model for a turbulently flowing suspension of solid spherical particles

Consider a stationary, homogeneous and isotropic turbulent flow field without particles. The velocity- and pressure field are, respectively, given by $\mathbf{v}_0$ and p_0. In order for the flow field to remain stationary, homogeneous and isotropic an external (stirring) force field $\mathbf{F}_0$ acts on the

fluid. N particles are then added to the fluid, keeping the force field $\mathbf{F}_0$. To calculate the new velocity field and pressure field, the method of induced forces can be employed. In this method the two-phase system is described by a velocity field $\mathbf{v}$, called the suspension velocity, which is identical to the fluid velocity in the part of space occupied by the fluid, and identical to the solid body motion of the particles in the part of space occupied by the particles. The effect of the stick boundary condition at the surfaces of the particles is represented by the force $\mathbf{F}$ acting on the fluid. The relation between the suspension velocity $\mathbf{v}$ and the unperturbed (without particles) fluid velocity $\mathbf{v}_0$ can formally be written in the following way (after Fourier transformation with respect to time)

$$\mathbf{v}_\omega(1,\ldots,N;\mathbf{r}) = \int \mathrm{d}r'\, \mathbf{K}_\omega\big(\mathbf{r},\mathbf{r}';1,\ldots,N\big)\cdot\mathbf{v}_{0,\,\omega}(\mathbf{r}'), \tag{1}$$

or briefly

$$\mathbf{v}_\omega(1,\ldots,N) = \mathbf{K}_\omega(1,\ldots,N)\cdot\mathbf{v}_{0,\,\omega}, \tag{2}$$

where ω is the frequency. Similarly, the relation between the force $\mathbf{F}$ and $\mathbf{v}_0$ can formally be written as

$$\mathbf{F}_\omega(1,\ldots,N) = \mathbf{A}_\omega(1,\ldots,N)\cdot\mathbf{v}_{0,\,\omega}. \tag{3}$$

(The calculation of the operators $\mathbf{K}_\omega$ and $\mathbf{A}_\omega$ will be discussed.) The probability distribution of the particles in the fluid flow field is given by $P(1,\ldots,N)$. Ensemble averaging of Eqs. (2) and (3) yields the average relations

$$\langle\mathbf{v}_\omega\rangle = \int\cdots\int \mathrm{d}\mathbf{R}_1\cdots\mathrm{d}\mathbf{R}_N\, P(1,\ldots,N)\mathbf{K}_\omega(1,\ldots,N)\cdot\mathbf{v}_{0,\,\omega}, \tag{4}$$

$$\langle\mathbf{F}_\omega\rangle = \int\cdots\int \mathrm{d}\mathbf{R}_1\cdots\mathrm{d}\mathbf{R}_N\, P(1,\ldots,N)\mathbf{A}_\omega(1,\ldots,N)\cdot\mathbf{v}_{0,\,\omega}, \tag{5}$$

where $\langle\mathbf{v}_\omega\rangle$ is the mean suspension velocity. In order to separate the fluid and particle motion, it is convenient to introduce the mean fluid velocity $\mathbf{v}_{\mathrm{f}\omega}$ and the mean particle velocity $\mathbf{v}_{\mathrm{p}\omega}$. These velocities are related to the mean suspension velocity by

$$\langle\mathbf{v}_\omega\rangle = (1-\phi)\mathbf{v}_{\mathrm{f}\omega} + \phi\mathbf{v}_{\mathrm{p}\omega}, \tag{6}$$

in which ϕ is the volume fraction of the particles. The plan is to eliminate $\mathbf{v}_{0,\,\omega}$ from Eqs. (4) and (5), and to derive the relation between $\langle\mathbf{F}_\omega\rangle$ and $\langle\mathbf{v}_\omega\rangle$

$$\langle\mathbf{F}_\omega\rangle = \chi^*_\omega\cdot\langle\mathbf{v}_\omega\rangle, \tag{7}$$

with χ^*_ω the effective friction operator, which has to be determined. For that purpose we first introduce cluster expansions for $\mathbf{K}_\omega(1,\ldots,N)$ and $\mathbf{A}_\omega(1,\ldots,N)$ in the relations Eqs. (4) and (5). These relations then become expansions with their terms ordered with respect to the number of particles involved. For Eq. (4) we introduce the cluster operators $\mathbf{L}_\omega$ defined in the following way

$$\mathbf{K}_\omega(\Phi) = \mathbf{L}_\omega(\Phi) = 1,$$

$$\mathbf{K}_\omega(1) = \mathbf{L}_\omega(1) + \mathbf{L}_\omega(\Phi),$$

$$\mathbf{K}(1, 2) = \mathbf{L}_\omega(1, 2) + \mathbf{L}_\omega(1) + \mathbf{L}_\omega(2) + \mathbf{L}_\omega(\Phi),$$

etc.

Above Φ is the empty set. For Eq. (5) we choose particle 1 as reference particle, and introduce so-called rooted cluster operators $\mathbf{M}_\omega$, defined as

$$\mathbf{A}_\omega(1) = \mathbf{M}_\omega(1),$$

$$\mathbf{A}(1, 2) = \mathbf{M}_\omega(1; 2) + \mathbf{M}_\omega(1),$$

etc.

Substituting the above expressions in Eqs. (4) and (5) gives, after some calculations,

$$\langle \mathbf{v}_\omega \rangle = \sum_{s=0}^{N} \frac{1}{s!} \int \cdots \int \mathrm{d}\mathbf{R}_1 \cdots \mathrm{d}\mathbf{R}_s \, n(1, \ldots, s) \mathbf{L}_\omega(1, \ldots, s) \cdot \mathbf{v}_{0,\,\omega} \tag{8}$$

$$\langle \mathbf{F}_\omega \rangle = \sum_{s=1}^{N} \frac{1}{(s-1)!} \int \cdots \int \mathrm{d}\mathbf{R}_1 \cdots \mathrm{d}\mathbf{R}_s \, n(1, \ldots, s) \mathbf{M}_\omega(1; 2, \ldots, s) \cdot \mathbf{v}_{0,\,\omega}, \tag{9}$$

in which $n(1, \ldots, s)$ is the partial probability distribution function defined as

$$n(1, \ldots, s) = \frac{N!}{(N-s)!} \int \cdots \int \mathrm{d}\mathbf{R}_{s+1} \cdots \mathrm{d}\mathbf{R}_N \, P(1, \ldots, N). \tag{10}$$

Elimination of $\mathbf{v}_{0,\,\omega}$ from Eqs. (8) and (9) gives the following first two terms in the expansion for the effective friction operator χ^*_ω

$$\chi^*_\omega = \int \mathrm{d}\mathbf{R}_1 \, n(1) \mathbf{M}_\omega(1) + \int \int \mathrm{d}\mathbf{R}_1 \, \mathrm{d}\mathbf{R}_2 \left[n(1, 2) \mathbf{M}_\omega(1; 2) - n(1) n(2) \mathbf{M}_\omega(1) \cdot \mathbf{L}_\omega(2) \right]. \tag{11}$$

$\mathbf{M}_\omega(1)$, $\mathbf{M}_\omega(1; 2)$ and $\mathbf{L}_\omega(2)$ can be calculated by solving the single-particle and two-particle flow problem. Felderhof and Ooms have done this in point-particle approximation using Stokes' resistance law for the particles. Felderhof and Jansen have solved the single-particle flow problem for the finite-diameter-particle case. They take the full force field exerted by the particle on the fluid into account (that is all force multipole moments, not only the first). In this way their model accounts implicitly for such terms in the particle equation of motion as the added-mass term and the Basset term, in addition to the friction term. Their calculation method can handle the two-particle flow problem in principle, but the calculations are very tedious and computationally intensive.

Substitution of Eq. (7) in the equation of motion gives (after spatial Fourier transformation) for the finite-diameter-particle case

$$\left[\eta\left(\alpha^2+q^2\right)-\chi^{\mathrm{T}}(q,\omega)\right]\langle\mathbf{v}_{\mathbf{q}\omega}\rangle=(1-\phi)\mathbf{F}^{\mathrm{T}}_{0\mathbf{q}\omega}, \tag{12}$$

which specifies the mean suspension velocity $\langle\mathbf{v}_{\mathbf{q}\omega}\rangle$ in response to the transversal component of the force $\mathbf{F}^{\mathrm{T}}_{0\mathbf{q}\omega}$. The symbol η denotes the dynamic viscosity of the fluid, q the wave number and $\mathbf{q}$ the wave vector. α is given by

$$\alpha=\left(\frac{-i\omega\rho_{\mathrm{f}}}{\eta}\right)^{1/2}, \tag{13}$$

where ρ_{f} is the fluid density. The function $\chi^{\mathrm{T}}(q,\omega)$ is the transversal component of the effective friction operator defined by

$$\chi^{*}_{\omega}=\chi^{\mathrm{L}}(q,\omega)\hat{\mathbf{q}}\,\hat{\mathbf{q}}+\chi^{\mathrm{T}}(q,\omega)\left(1-\hat{\mathbf{q}}\,\hat{\mathbf{q}}\right), \tag{14}$$

in which $\hat{\mathbf{q}}$ is the unit vector in the direction of $\mathbf{q}$. For an incompressible fluid the pressure term does not occur in the equation of motion for the transversal component of the force. It is in the equation for the lateral component.

$\mathbf{F}^{\mathrm{T}}_{0\mathbf{q}\omega}$ can also be related to the mean unperturbed (without particles) fluid velocity field $\mathbf{v}_{0\mathbf{q}\omega}$ by means of the following expression

$$\left[\eta\left(\alpha^2+q^2\right)\right]\mathbf{v}_{0\mathbf{q}\omega=}\mathbf{F}^{\mathrm{T}}_{0\mathbf{q}\omega}. \tag{15}$$

Substitution of Eq. (15) into (12) yields the relation between the suspension velocity and the unperturbed fluid velocity

$$\langle\mathbf{v}_{\mathbf{q}\omega}\rangle=(1-\phi)H(q,\omega)\mathbf{v}_{0\mathbf{q}\omega}, \tag{16}$$

where the function $H(q,\omega)$ is given by

$$H(q,\omega)=\frac{\eta\left(\alpha^2+q^2\right)}{\eta\left(\alpha^2+q^2\right)-\chi^{\mathrm{T}}(q,\omega)}. \tag{17}$$

Straightforward calculations yield similar relations for the mean particle velocity $\mathbf{v}_{\mathrm{p}\mathbf{q}\omega}$ and the mean fluid velocity $\mathbf{v}_{\mathrm{f}\mathbf{q}\omega}$ for the finite-diameter-particle case in terms of $\mathbf{v}_{0\mathbf{q}\omega}$ and $p_{0\mathbf{q}\omega}$

$$\mathbf{v}_{\mathrm{p}\mathbf{q}\omega}=\left\{\left[(1-\phi)\Gamma^{\mathrm{T}}(q,\omega)\right]H(q,\omega)+\Gamma^{\mathrm{T}}_{F}(q,\omega)\eta\left(\alpha^2+q^2\right)\right\}\mathbf{v}_{0\mathbf{q}\omega}+\Gamma^{\mathrm{L}}_{F}(q,\omega)i\mathbf{q}p_{0\mathbf{q}\omega}, \tag{18}$$

$$\mathbf{v}_{\mathrm{f}\mathbf{q}\omega} = \left\{\left[1 - \phi\Gamma^{\mathrm{T}}(q,\omega)\right]H(q,\omega) - \frac{\phi}{1-\phi}\Gamma_F^{\mathrm{T}}(q,\omega)\eta\left(\alpha^2 + q^2\right)\right\}\mathbf{v}_{0\mathbf{q}\omega}$$

$$- \frac{\phi}{1-\phi}\Gamma_F^{\mathrm{L}}(q,\omega)i\mathbf{q}p_{0\mathbf{q}\omega}, \tag{19}$$

The functions $\chi^{\mathrm{T}}(q,\omega)$, $\Gamma^{\mathrm{T}}(q,\omega)$, $\Gamma_F^{\mathrm{L}}(q,\omega)$ and $\Gamma_F^{\mathrm{L}}(q,\omega)$ are specified in Appendix A.

Within the point-particle approach the force density $\mathbf{F}_{0\mathbf{q}\omega}^{\mathrm{T}}$ acts in the entire space, whereas in the finite-diameter-particle approach its action is restricted to the space occupied by the fluid. Accordingly, Eq. (12) differs for the point-particle case by the fact that the factor $(1-\phi)$ on the right-hand side is absent. The equivalent of Eq. (16) is therefore given by

$$\langle\mathbf{v}_{\mathbf{q}\omega}\rangle = H(q,\omega)\mathbf{v}_{0\mathbf{q}\omega}, \tag{20}$$

where the function $H(q,\omega)$ is as in Eq. (17). Within the point-particle approach the mean fluid velocity $\mathbf{v}_{\mathrm{f}\mathbf{q}\omega}$ is identical to the suspension velocity $\langle\mathbf{v}_{\mathbf{q}\omega}\rangle$

$$\mathbf{v}_{\mathrm{f}\mathbf{q}\omega} = \langle\mathbf{v}_{\mathbf{q}\omega}\rangle = H(q,\omega)\mathbf{v}_{0\mathbf{q}\omega}, \tag{21}$$

while the mean particle velocity field $\mathbf{v}_{\mathrm{p}\mathbf{q}\omega}$ can be expressed as

$$\mathbf{v}_{\mathrm{p}\mathbf{q}\omega} = \Gamma^{\mathrm{T}}(q,\omega)\langle\mathbf{v}_{\mathbf{q}\omega}\rangle = \Gamma^{\mathrm{T}}(q,\omega)H(q,\omega)\mathbf{v}_{0\mathbf{q}\omega}. \tag{22}$$

$\Gamma^{\mathrm{T}}(q,\omega)$ and $\chi^{\mathrm{T}}(q,\omega)$ for the point-particle approach are different from their expressions for the finite-diameter-particle approach, as in the point-particle approach the hydrodynamic interactions between the particles (in two-particle approximation) are taken into account. They are specified in Appendix B.

3. Calculation method for turbulence intensities

In the foregoing paragraphs we described the dynamics of a solid spheres suspension for an arbitrary space- and time-dependent driving force field $\mathbf{F}_0(\mathbf{r},t)$. The response of the suspension was evaluated in the temporal and spatial Fourier domain. The resulting suspension velocity field $\langle\mathbf{v}_{\mathbf{q}\omega}\rangle$, the particle velocity field $\mathbf{v}_{\mathrm{p}\mathbf{q}\omega}$ and the perturbed fluid velocity field $\mathbf{v}_{\mathrm{f}\mathbf{q}\omega}$ were determined in the finite-diameter-particle approach and the point-particle approach.

In this section, we choose a specific unperturbed fluid velocity field $\mathbf{v}_0$ that shows the features of isotropic, homogeneous, stationary turbulence and calculate the perturbed (with particles) fluid and particle velocity fields.

The velocity field $\mathbf{v}_0$ will be regarded as a stochastic velocity field described by

$$\overline{\mathbf{v}_0(\mathbf{r},t)\mathbf{v}_0(\mathbf{r}',t')} = \Gamma_0\left(\mathbf{r}-\mathbf{r}',t-t'\right), \tag{23}$$

where the bar indicates an average over an ensemble of realizations of the turbulent velocity field. The correlation Γ_0 depends on the relative position $\mathbf{r}-\mathbf{r}'$ and relative time $t-t'$ only and is independent of the absolute spatial and time coordinates. Fourier transforming equation (23) yields

$$\overline{\mathbf{v}_{0\mathbf{q}\omega}\mathbf{v}^{*}_{0\mathbf{q}'\omega'}} = \frac{1}{(2\pi)^8}\int \mathrm{d}\mathbf{r}\,\mathrm{d}t\,\mathrm{d}\mathbf{r}'\,\mathrm{d}t'\,\overline{\mathbf{v}_0(\mathbf{r},t)\mathbf{v}_0(\mathbf{r}',t')}\mathrm{e}^{i(\omega t-\mathbf{q}\cdot\mathbf{r})}\mathrm{e}^{-i\left(\omega' t'-\mathbf{q}'\cdot\mathbf{r}'\right)}$$

$$= \mathbf{S}_0(\mathbf{q},\omega)\delta\left(\mathbf{q}-\mathbf{q}'\right)\delta(\omega-\omega'), \tag{24}$$

where the $(*)$ denotes the complex conjugate. The spectral tensor field $\mathbf{S}_0(\mathbf{q},\omega)$ is defined as

$$\mathbf{S}_0(\mathbf{q},\omega) = \frac{1}{(2\pi)^4}\int \mathrm{d}\boldsymbol{r}\int \mathrm{d}t\,\Gamma_0(\mathbf{r},t)\mathrm{e}^{i(\omega t-\mathbf{q}\cdot\mathbf{r})}. \tag{25}$$

The fluid is assumed to be incompressible. For this reason $\mathbf{S}_0(\mathbf{q},\omega)$ is purely transversal and can be written as

$$\mathbf{S}_0(\mathbf{q},\omega) = S_0(q,\omega)\left(\mathbf{I}-\hat{\mathbf{q}}\,\hat{\mathbf{q}}\right). \tag{26}$$

The quantity $S_0(q,\omega)$ is referred to as the unperturbed (without particles) spectral density of the fluid.

We assume the following form for the unperturbed spectral density

$$S_0(q,\omega) = \frac{E_0(q)}{4\pi q^2}R_0(q,\omega), \tag{27}$$

where $E_0(q)$ represents the three-dimensional energy wavenumber distribution and $R_0(q,\omega)$ is the corresponding relaxation function. These functions should fulfil the conditions

$$\int_0^\infty \mathrm{d}q\,E_0(q) = \frac{1}{2}\overline{v_0^2}, \quad \int_{-\infty}^{\infty}\mathrm{d}\omega\,R_0(q,\omega) = 1. \tag{28}$$

The last property expresses the fact that the turbulent energy contained in the eddies with a wavenumber between q and $q+\mathrm{d}q$ is constant in time, as is required for stationary turbulence. This implies that, for each wavenumer q the energy added by the force density field $\mathbf{F}^{\mathrm{T}}_{0\mathbf{q}\omega}$ is exactly balanced by viscous dissipation. For $E_0(q)$ the following distribution, given by Hinze (1975), p. 211, is assumed

$$E_0(q) = \frac{8}{3\pi}\overline{v_0^2}\frac{q^4\Lambda^5}{\left(1+q^2\Lambda^2\right)^3}, \tag{29}$$

which corresponds to an exponential decay of the longitudinal correlation function. The quantity Λ is called the Eulerian integral length scale. It can be shown that the relaxation function $R_0(q,\omega)$ is equal to

$$R_0(q,\omega) = \frac{1}{\pi}\frac{\nu q^2}{\omega^2+\left(\nu q^2\right)^2}. \tag{30}$$

The chosen functions $E_0(q)$ and $R_0(q,\omega)$ fulfil the conditions of Eq. (28). This implies that

$$\int_0^\infty \mathrm{d}q\, 4\pi q^2 \int_{-\infty}^{\infty} \mathrm{d}\omega\, S_0(q,\omega) = \frac{1}{2}\overline{v_0^2} = k_0, \tag{31}$$

where k_0 is defined as the turbulence intensity of the fluid in the absence of particles.

Given the unperturbed spectral density $S_0(q,\omega)$, the perturbed fluid spectral density $S_\mathrm{f}(q,\omega)$ and the particle spectral density $S_\mathrm{p}(q,\omega)$ can be derived using the Eqs. (19) and (18) for the fluid velocity field and the particle velocity field, respectively, in case of the finite-diameter-particle approach. In this derivation also the following relations are used

$$\mathbf{F}^\mathrm{L}_{0\mathbf{q}\omega} = i\mathbf{q}p_{0\mathbf{q}\omega} \tag{32}$$

and

$$\overline{|\mathbf{F}^\mathrm{L}_{0\mathbf{q}\omega}|^2} = \frac{1}{2}\overline{|\mathbf{F}^\mathrm{T}_{0\mathbf{q}\omega}|^2}, \tag{33}$$

which hold for isotropic flows and which relates the unperturbed fluid pressure to the unperturbed fluid velocity. This yields after straightforward calculations

$$S_\mathrm{f}(q,\omega) = \left\{ \left| \left[1 - \phi\Gamma^\mathrm{T}(q,\omega)\right] H(q,\omega) - \frac{\phi}{1-\phi}\tilde{\Gamma}^\mathrm{T}_F(q,\omega) \right|^2 + \frac{1}{2}\left(\frac{\phi}{1-\phi}\right)^2 |\tilde{\Gamma}^\mathrm{L}_F(q,\omega)|^2 \right\} S_0(q,\omega) \tag{34}$$

$$S_\mathrm{p}(q,\omega) = \left\{ |\Gamma^\mathrm{T}(q,\omega)(1-\phi)H(q,\omega) + \tilde{\Gamma}^\mathrm{T}_F(q,\omega)|^2 + \frac{1}{2}|\tilde{\Gamma}^\mathrm{L}_F(q,\omega)|^2 \right\} S_0(q,\omega), \tag{35}$$

where

$$\tilde{\Gamma}^\mathrm{T}_F(q,\omega) = \eta\left(\alpha^2 + q^2\right)\Gamma^\mathrm{T}_F(q,\omega), \quad \tilde{\Gamma}^\mathrm{L}_F(q,\omega) = \eta\left(\alpha^2 + q^2\right)\Gamma^\mathrm{L}_F(q,\omega). \tag{36}$$

With Eqs. (34) and (35) the relevant spectra can be calculated from the spectrum of the unperturbed fluid in the finite-diameter-particle approach.

For the point-particle approach it can easily be shown that these equations can be written in the following form

$$S_\mathrm{f} = |H(q,\omega)|^2 S_0(q,\omega) \tag{37}$$

$$S_\mathrm{p} = |\Gamma^\mathrm{T}(q,\omega)|^2 |H(q,\omega)|^2 S_0(q,\omega). \tag{38}$$

Now the calculation of the spectra (in finite-diameter-particle- and point-particle approximation) has been specified, the calculation scheme for the turbulence intensities can be finalized. Analogous to the quantity $k_0 = \frac{1}{2}\overline{v_0^2}$ of Eq. (31) the following turbulence intensities can be introduced

$$k_\mathrm{f} = \frac{1}{2}\overline{v_\mathrm{f}^2} = \int_0^\infty \mathrm{d}q\, 4\pi q^2 \int_{-\infty}^{\infty} \mathrm{d}\omega\, S_\mathrm{f}(q,\omega) \tag{39}$$

$$k_p = \frac{1}{2}\overline{v_p^2} = \int_0^\infty dq\, 4\pi q^2 \int_{-\infty}^{\infty} d\omega\, S_p(q, \omega). \tag{40}$$

We define the ratio of the turbulence intensities of the perturbed (with particles) flow and the unperturbed (without particles) flow

$$k_f/k_0, \tag{41}$$

and the ratio of the turbulence intensities of the particles and the perturbed fluid flow

$$k_p/k_f. \tag{42}$$

In the next section, results will be given for these two ratios as function of relevant dimensionless groups, using the calculation scheme developed above. Both the results derived with the finite-diameter-particle approach and the point-particle approach will be presented and compared.

4. Results, comparison with other studies and conclusions

When formulating the resulting equations of the previous paragraphs in a dimensionless way, three dimensionless parameters appear, viz. ϕ, ρ_f/ρ_p and a/Λ. (ϕ is the particle volume fraction, ρ_f is the fluid density, ρ_p is the particle density, a is the particle diameter and Λ is the integral length scale of turbulence.) So, in this section, results will be presented in a dimensionless form as function of these three parameters. A set of Matlab programs was developed for the numerical calculation of the spectra, the turbulence intensities and their ratios k_f/k_0 and k_p/k_f. (The Matlab programs are available on request.) The different models that were discussed (namely the finite-diameter-particle model without hydrodynamic interaction between the particles, and the point-particle model with and without hydrodynamic interaction) can be applied with these programs.

The turbulence intensities k_0, k_f and k_p are obtained by integration of the corresponding spectral densities over the full q, ω-domain (see Eqs. (31), (39) and (40)). The turbulence intensity ratios k_f/k_0 and k_p/k_f are plotted in Figs. 1 and 2 as function of the dimensionless particle diameter a/Λ for a particle volume fraction $\phi = 0.1$ and a density ratio $\rho_f/\rho_p = 10.$. In Figs. 3 and 4, these ratios are plotted as function of a/Λ for a particle volume fraction $\phi = 0.1$ and a density ratio $\rho_f/\rho_p = 1$. ($\rho_f/\rho_p = 1$ means that the particle density is the same as the fluid density.) Finally, in Figs. 5 and 6, the turbulence intensity ratios are plotted as function of a/Λ for a particle volume fraction $\phi = 0.1$ and a density ratio $\rho_f/\rho_p = 0.01$. The range of a/Λ-values is between 10^{-3} and about 10^{-1}. For larger values other phenomenons, such as turbulence generation in the wake of the particles, become important. Such phenomenons are not incorporated in the physical model. (Sometimes it is claimed that the effect of the wake of the particles becomes already noticeable for values of the ratio of the particle diameter and the integral length scale larger than 0.01. If that is true, only the results given in Figs. 1–6 for values of a/Λ smaller than 0.01 have physical meaning.)

A number of important conclusions can be drawn from the results given in the figures. First of all, it is clear that at a volume fraction $\phi = 0.1$ the particles can already have a significant

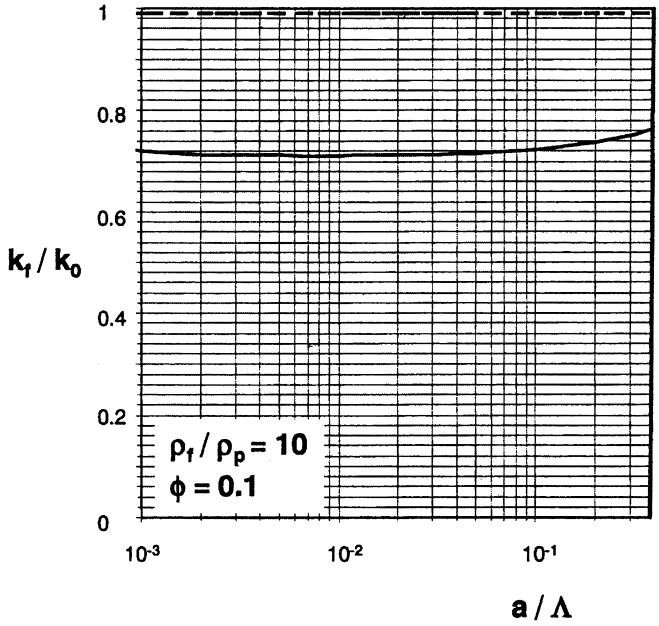

Fig. 1. k_f/k_0 as function of a/Λ for density ratio $\rho_f/\rho_p = 10$ evaluated for the finite-diameter-particle case (———), and for the point-particle case with (.....) and without (– – –) hydrodynamic interaction.The results found in point-particle approximation with and without hydrodynamic interaction practically coincide.

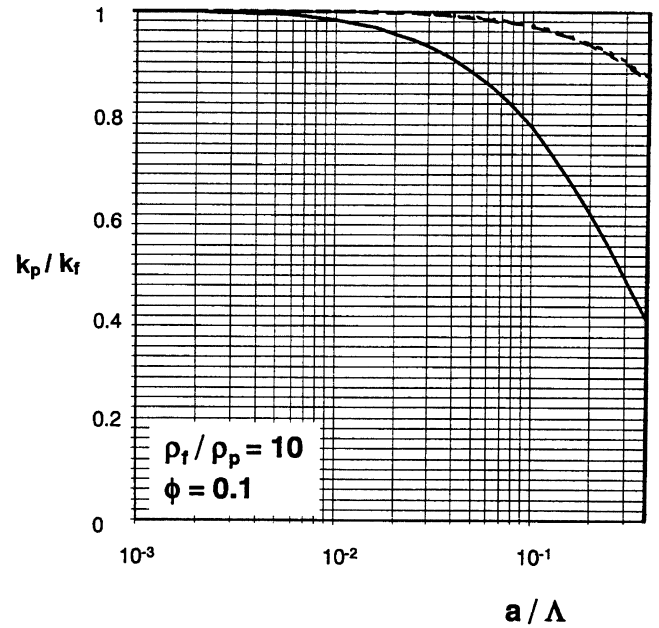

Fig. 2. k_p/k_f as function of a/Λ for density ratio $\rho_f/\rho_p = 10$ evaluated for the finite-diameter particle case (———), and for the point-particle case with (.....) and without (– – –) hydrodynamic interaction. The results found in point-particle approximation with and without hydrodynamic interaction practically coincide.

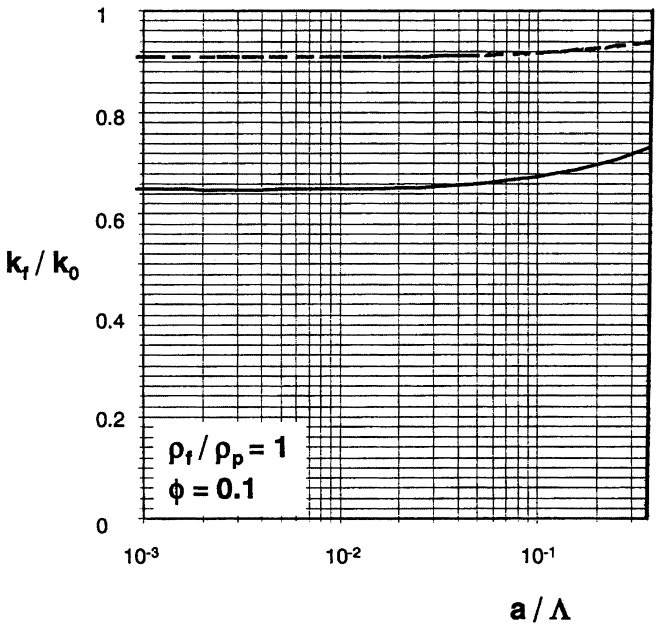

Fig. 3. k_f/k_0 as function of a/Λ for density ratio $\rho_f/\rho_p = 1$ evaluated for the finite-particle-particle case (———), and for the point-particle case with (.....) and without (– – –) hydrodynamic interaction. The results found in point-particle approximation with and without hydrodynamic interaction practically coincide.

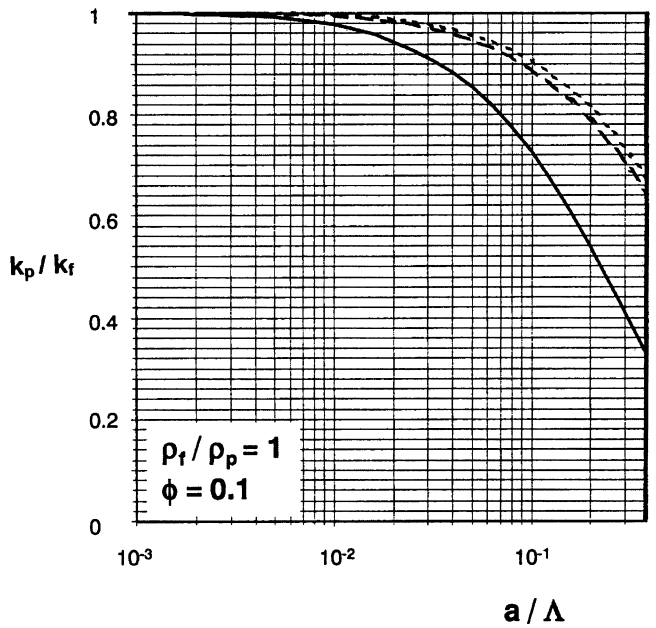

Fig. 4. k_p/k_f as function of a/Λ for density ratio $\rho_f/\rho_p = 1$ evaluated for the finite-diameter-particle case (———), and for the point-particle case with (.....) and without (– – –) hydrodynamic interaction.

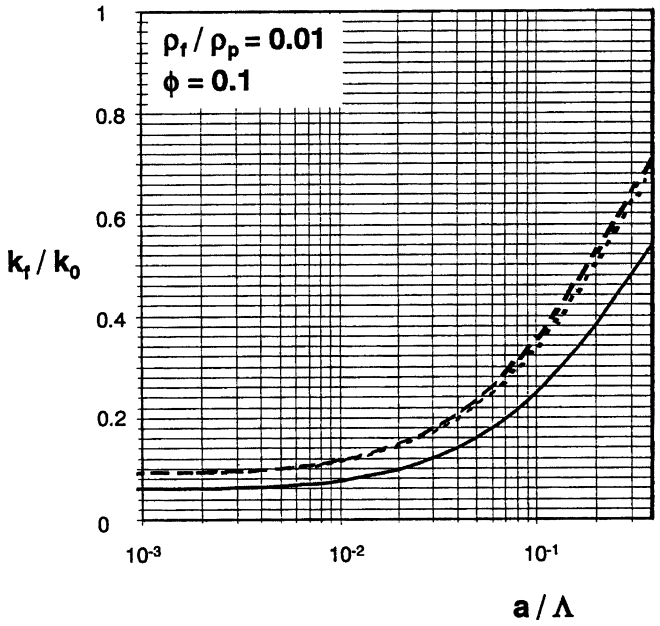

Fig. 5. k_f/k_0 as function of a/Λ for density ratio $\rho_f/\rho_p = 0.01$ evaluated for the finite-diameter-particle case (———), and for the point-particle case with (. . . . .) and without (– – –) hydrodynamic interaction.

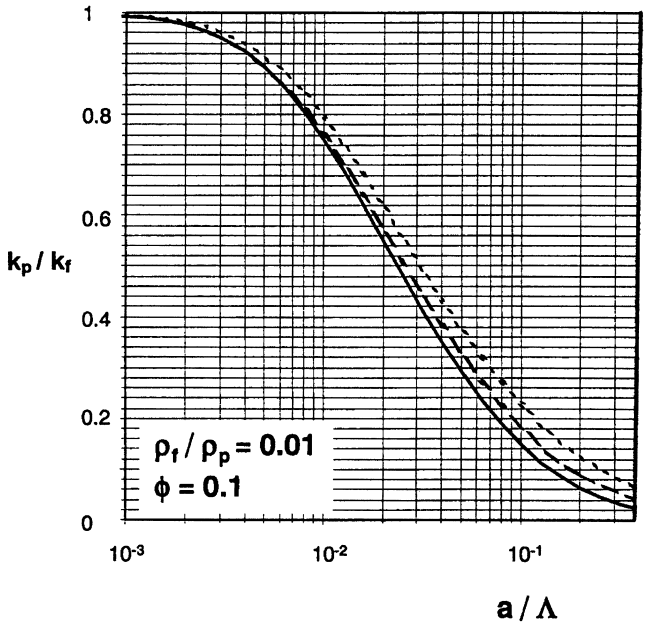

Fig. 6. k_p/k_f as function of a/Λ for density ratio $\rho_f/\rho_p = 0.01$ evaluated for the finite-diameter-particle case (———), and for the point-particle case with (. . . . .) and without (– – –) hydrodynamic interaction.

influence on the fluid turbulence. This influence increases with decreasing value of ρ_f/ρ_p. For $\rho_f/\rho_p = 0.01$, the fluid turbulence intensity can even be reduced to a value less than 10% of the turbulence intensity of the fluid without particles. So this influence has to be taken into account for a realistic modeling of turbulent dispersed fluid–solid flows. It can be seen from the figures that at the same volume fraction smaller particles are more effective in suppressing the fluid turbulence than larger particles. The reason is that at the same volume fraction smaller particles have a larger surface area and cause more friction with the fluid than larger particles. Secondly, the effect of the hydrodynamic interactions at $\phi = 0.1$ is still mostly negligible (at least in point-particle approximation). Only at very low values of the density ratio ρ_f/ρ_p the hydrodynamic interactions become significant. This conclusion is important, as the calculation of the hydrodynamic interaction between particles is quite cumbersome. Finally, the differences between the results for the point-particle model and the finite-diameter-particle model are, in general, significant for all values of a/Λ. So one has to be careful with point-particle models.

A comparison has been made with the results of other studies, mentioned in Section 1. Below the comparison with two of these studies, viz. the study by Squires and Eaton (1990) and Yarin and Hetsroni (1994), will be discussed.

Squires and Eaton, using direct numerical simulation, investigated also the turbulence modification by particles in stationary, homogeneous, isotropic turbulence. It has to be pointed out that they did not calculate the detailed flow around finite-diameter particles. They included the Stokes force of the particles on the fluid as point forces in the equation of motion. They found that the effect of increased mass loading is to suppress the fluid turbulence intensity by about 10% (mass loading = 0.1) to about 50% (mass loading = 1.0). This is in reasonable agreement with our results given in Fig. 1 (mass loading = 0.01), Fig. 3 (mass loading = 0.1) and Fig. 5 (mass loading = 10). It can be seen from these figures that dependent on the particle size and on the version of the model (point-particle model or finite-diameter-particle model), the decrease in the fluid turbulence intensity goes from a few percent to almost 90% with increasing mass loading. Squires and Eaton also studied the effect of the particles on the fluid turbulence spectrum. They found that as the mass loading is increased the energy in the low wavenumbers (large eddies) decreases relative to the energy in the high wavenumbers (small eddies). (As discussed, the total energy of all eddies decreases with increasing mass loading.) The same result is found with the model described in this publication. In Fig. 7, the ratio of the fluid turbulence spectra with and without particles S_f/S_0 (calculated with the point-particle model) is shown as function of the dimensionless wavenumber qa and the dimensionless frequency $\omega a^2/\nu$ for $\phi = 0.1$ and $\rho_f/\rho_p = 0.01$, a is the particle diameter and ν is the kinematic viscosity of the fluid. At small wavenumbers and low frequencies the particles follow the motion of the fluid and the suspension has an effective mass density $\rho_s = \rho_f + \phi\rho_p$. This strongly reduces the fluid turbulence spectrum at these wavenumbers and frequencies. Squires and Eaton found that at low mass loadings the particles are not uniformly dispersed throughout the fluid volume and that there are distinct regions of particles accumulation. This effect is not incorporated in our model. However, they point out that an optimum ratio of particle time scale and fluid turbulence time scale must exist for strong preferential concentrations to occur. Moreover, according to them the increased coupling between the

particles and the fluid turbulence at higher mass loadings reduces the tendency for particles to accumulate in distinct regions.

As discussed, Yarin and Hetsroni developed a theoretical model for the particles–turbulence interaction that takes into account the fluid turbulence suppression by the particles and the fluid turbulence generation in the wake behind particles. In our model, only the fluid turbulence suppression is considered; we hope to include the turbulence generation in future work. For small particles the turbulence generation is negligible, and so in that case it is possible to compare the results of our model with those given in Yarin and Hetsroni's publication. After dimensional analysis they derive the following four relevant dimensionless groups: a/Λ, ρ_f/ρ_p, $\phi(\rho_p/\rho_f)$ (the particle mass loading) and Re_p (the particle Reynolds number). In our model we find only the first three dimensionless groups, the particle Reynolds number is absent. The reason is that Yarin and Hetsroni use a Reynolds-number dependent resistance law for the particles, whereas we use in the point-particle model Stokes' law and in the finite-diameter-particle model restrict ourselves to a low Reynolds number flow. The particle Reynolds number would, of course, also be present in our model, when we would use, for instance, the particle resistance law of Yarin and Hetsroni in the point-particle model. Yarin and Hetsroni mention in their publication that for small particles the particles–turbulence interaction is determined by only one parameter: the mass content of the particles in the suspension $(\rho_p/\rho_f)\phi$. We checked this statement analytically in our point-particle model, and indeed found that for small values $\omega a^2/\nu$ and for negligible hydrodynamic interaction between the particles, the turbulence modification is dependent on the combined parameter $(\rho_p/\rho_f)\phi$ and not on ρ_f/ρ_p and ϕ separately. However, for larger values of $\omega a^2/\nu$ this statement can no longer be valid. Our results for the turbulence modification for small particles agree reasonably well with the results of Yarin and Hetsroni in case of the point particle model. For large values of the particle mass loading the results of the finite-diameter-particle model also agree reasonably well. However, for small values of the particle mass loading but finite values of the particle volume fraction (ϕ has a finite value; ρ_p/ρ_f is small), there is a remarkable difference between the finite-diameter-particle model, on the one hand, and the point-particle model and the model of Yarin and Hetsroni,

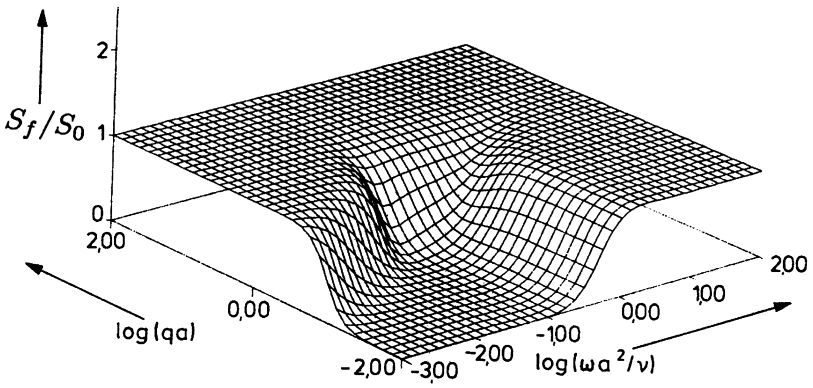

Fig. 7. S_f/S_0 as function of qa and $\omega a^2/\nu$ for $\phi = 0.1$ and $\rho_f/\rho_p = 0.01$ evaluated for the point-particle case with hydrodynamic interaction.

on the other. (This difference can also clearly be seen in Fig. 1.) For small particle mass loading, the effect of the particles on the fluid turbulence intensity is negligible according to the point-particle model and the Yarin–Hetsroni model. However, as long as ϕ remains finite ($\phi = 0.1$ in Fig. 1) there remains a considerable damping effect of the particles on the fluid turbulence according to the finite-diameter-particle model. We plan to carry out experiments to check this interesting result.

5. Suggestions for future research

In order to extend the scope of the work presented in this publication and to verify the sensitivity on some of the underlying assumptions, it would be useful to investigate the following items:

1. Dependence on the choice of the unperturbed turbulence spectrum. The turbulence intensities presented in this publication are derived on the basis of the assumed unperturbed spectral density $S_0(q, \omega)$, defined by Eqs. (27), (29) and (30). The slow decay for large values of q is probably not realistic and requires modification for values of q in the range of the Kolmogorov length scale. Moreover, the distribution does not exhibit the $q^{-5/3}$-behavior that is characteristic for eddies with length scales in the inertial subrange. It would be interesting to repeat the calculations of this publication with one or more different unperturbed spectral densities $S_0(q, \omega)$ and to study the sensitivity of the results with respect to the shape of the spectrum. Next to the three dimensionless groups discussed earlier (ϕ, ρ_f/ρ_p and a/Λ), another dimensionless group (the ratio of the Kolmogorov length scale and the integral length scale) will then occur in the model.
2. Crossing trajectory effect. The presence of a uniform external force acting on the particles (such as the gravity force) affects the particle velocity and, therefore, also the fluid turbulence. The reason is that the residence time of a particle in a certain fluid eddy is shortened as a result of its motion in the direction of the external force. This effect is known as the crossing trajectory effect. Since the gravity force is indeed present in all systems of interest, it is worthwhile investigating the modifications of the physical model when an additional constant term is included in the equation of motion.

The above two extensions of our model are very well possible. Other topics such as turbulence generation by the particles, wall effects and particle dispersion are also important but are not simple extensions of the present work.

Acknowledgements

The authors are grateful to W.M.M. Schinkel for his support in the development of the Matlab-programs.

Appendix A. Specification of $\chi^{T}(q,\omega)$, $\Gamma^{T}(q,\omega)$, $\Gamma_F^{T}(q,\omega)$ and $\Gamma_F^{L}(q,\omega)$ for finite-diameter-particle case

It is convenient to introduce the dimensionless arguments x and y which are related to ω and q, respectively, in the following way:

$$x = \alpha a, \quad y = qa, \tag{A1}$$

where a is the diameter of the particles. The functions $\chi^{T}(q,\omega)$, $\Gamma^{T}(q,\omega)$, $\Gamma_F^{T}(q,\omega)$ and $\Gamma_F^{L}(q,\omega)$ were determined by Felderhof and Jansen and are given by (see also Felderhof and Jansen, 1991, paragraphs 5 and 6)

$$\chi^{T}(q,\omega) = \frac{3}{2}\frac{\phi}{a^2}\eta\left[P_{01}(q,\omega) + P_{U1}(q,\omega) + P_{\Omega 1}(q,\omega)\right] \tag{A2}$$

$$\Gamma^{T}(q,\omega) = 3\frac{j_1}{y}\gamma_t(q,\omega) + \frac{3}{2}j_2\gamma_r(q,\omega) \tag{A3}$$

$$\Gamma_F^{T}(q,\omega) = -4\pi a^3\frac{j_1}{y}y_t(q,\omega) - \frac{4}{5}\pi a^5 j_2 y_r(q,\omega) \tag{A4}$$

$$\Gamma_F^{L}(q,\omega) = -4\pi a^3\frac{j_1}{y}y_t(q,\omega), \tag{A5}$$

where

$$P_{01}(q,\omega) = -3(1+x)j_0^2 - \sum_{l=1}^{\infty}\left\{l(2l+1)\frac{x^2+y^2}{y^2} + \frac{x}{k_l}\left[(2l+3)k_{l+1} + (2l+1)k_{l-1}\right]\right\}j_l^2 \tag{A6}$$

$$P_{U1}(q,\omega) = \left[3(1+x)j_0 + 3x^2\frac{j_1}{y}\right]\tilde{\gamma}_t(q,\omega) \tag{A7}$$

$$P_{\Omega 1}(q,\omega) = \left[\frac{3+3x+x^2}{1+x}yj_1 + x^2 j_2\right]\tilde{\gamma}_r(q,\omega), \tag{A8}$$

in which

$$\tilde{\gamma}_t(q,\omega) = \gamma_t(q,\omega) - \frac{4\pi}{3}\eta a\left(x^2+y^2\right)y_t(q,\omega) \tag{A9}$$

$$\tilde{\gamma}_r(q,\omega) = \frac{y}{2a}\left[\gamma_r(q,\omega) - \frac{8\pi}{15}\eta a^3\left(x^2+y^2\right)y_r(q,\omega)\right]. \tag{A10}$$

The functions g_l (which will be used later on) and k_l are modified spherical Bessel functions

taken at argument x and the functions j_l are spherical Bessel functions of the first kind taken at argument y. They are defined as

$$g_l = \left(\frac{\pi}{2x}\right)^{\frac{1}{2}} I_{l+\frac{1}{2}}(x), \quad k_l = \left(\frac{\pi}{2x}\right)^{\frac{1}{2}} K_{l+\frac{1}{2}}(x), \quad j_l = \left(\frac{\pi}{2y}\right)^{\frac{1}{2}} J_{l+\frac{1}{2}}(x), \tag{A11}$$

where J_n is the Bessel function of the first kind and order n, and I_n and K_n are modified Bessel functions of order n and of the first and second kind, respectively. Finally, the functions $y_t(q, \omega)$, $y_r(q, \omega)$, $\gamma_t(q, \omega)$ and $\gamma_r(q, \omega)$ need to be specified (see also Felderhof and Jansen, 1991, paragraph 6). The function $y_t(q, \omega)$ is defined by

$$y_t(q, \omega) = 3\frac{j_1}{y} y_t(\omega), \tag{A12}$$

where $y_t(\omega)$ is equal to

$$y_t(\omega) = \frac{1}{6\pi\eta a} \frac{1}{1 + x + \frac{1}{9}(1 + 2R_m)x^2}, \tag{A13}$$

in which R_m is the ratio of the particle density and the fluid density ρ_p/ρ_f. The function $y_r(q, \omega)$ is defined by

$$y_r(q, \omega) = \frac{15}{x^2 + y^2}\left(\frac{x g_0}{g_1}\frac{j_1}{y} - j_0\right) y_r(\omega), \tag{A14}$$

with $y_r(\omega)$ equal to

$$y_r(\omega) = \frac{1}{8\eta a^3} \frac{1 + x}{1 + x + \frac{1}{3} + \frac{1}{15}R_m(x^2 + x^3)}. \tag{A15}$$

The function $\gamma_t(q, \omega)$ is given by

$$\gamma_t(q, \omega) = \gamma_t(\omega) j_0 + \delta_t(\omega) j_2, \tag{A16}$$

where $\gamma_t(\omega)$ and $\delta_t(\omega)$ are defined as

$$\gamma_t(\omega) = \frac{1 + x + \frac{1}{3}x^2}{1 + x + Zx^2}, \quad \delta_t(\omega) = \frac{\frac{1}{3}x^2}{1 + x + Zx^2}, \tag{A17}$$

in which $Z = \frac{1}{9}(1 + 2R_m)$. Finally, the function $\gamma_r(q, \omega)$ is given by

$$\gamma_r(q, \omega) = 3\frac{j_1}{y} \gamma_r(\omega), \tag{A18}$$

with

$$\gamma_r(\omega) = \frac{xe^x}{3g_1}\frac{1}{1 + x + \frac{1}{3}x^2 + \frac{1}{15}R_m(x^2 + x^3)}. \tag{A19}$$

Appendix B. Specification of $\chi^T(q, \omega)$ and $\Gamma^T(q, \omega)$ for the point-particle case

For point particles with hydrodynamic interactions Felderhof and Ooms found

$$\chi^T(q, \omega) = -\phi\eta\alpha^2 R_m \Gamma^T(q, \omega), \tag{B1}$$

with

$$\Gamma^T(q, \omega) = \frac{1}{1 + \frac{2}{9}x^2 R_m\left[1 - \phi J(q, \omega)\right]}. \tag{B2}$$

The factor $J(q, \omega)$ represents the hydrodynamic interactions and is given by

$$J(q, \omega) = J_1(q, \omega) + J_2(q, \omega), \tag{B3}$$

where

$$J_1(q, \omega) = 3x\int_0^2 \mathrm{d}s\, s^2\left[A_1(ys)f(xs) + A_2(ys)g(xs)\right] \tag{B4}$$

$$J_2(q, \omega) = x^2\lambda\left(ix^2R_m\right)\int_2^\infty \mathrm{d}s\, s^2\left[\frac{1 - 3x\lambda\left(ix^2R_m\right)A_1(ys)f(xs)}{1 - x^2\lambda\left(ix^2R_m\right)f(xs)^2}f(xs)^2 + \frac{2 - 3x\lambda\left(ix^2R_m\right)A_2(ys)g(xs)}{1 - x^2\lambda\left(ix^2R_m\right)g(xs)^2}g(xs)^2\right], \tag{B5}$$

in which the quantities x and y are defined in Eq. (A1) and the functions f, g, A_1, A_2 and λ are given by

$$f(z) = \frac{3}{z^3}\left[1 - (1 + z)e^{-z}\right] \tag{B6}$$

$$g(z) = \frac{3}{2z^3}\left[-1 + \left(1 + z + z^2\right)e^{-z}\right] \tag{B7}$$

$$A_1(z) = \frac{\sin z - z\cos z}{z^3} \tag{B8}$$

$$A_2(z) = \frac{-\sin z + z\cos z + z^2 \sin z}{z^3} \tag{B9}$$

$$\lambda(z) = \frac{1}{1 + i\frac{9}{2z}}, \tag{B10}$$

where the argument z is, in general, a complex number. The effect of the hydrodynamic interactions can be omitted by taking the factor $[1 - \phi J(q, \omega)]$ out of Eq. (B2).

References

Crowe, C.T., Troutt, T.R., Chung, J.N., 1996. Numerical models for two-phase turbulent flows. Annual Rev. Fluid Mech 28, 11–43.

Crowe, C.T., Sommerfeld, M., Tsuji, Y., 1998. Multiphase Flows with Droplets and Particles. CRC Press, New York.

Elgobashi, S.E., Abou-Arab, T.W., 1983. A two-equation turbulence model for two-phase flow. Phys. Fluids 26, 931–938.

Elgobashi, S., Truesdell, G.C., 1993. On the two-way interaction between homogeneous turbulence and dispersed solid particles. Part I: Turbulence modification. Phys. Fluids 5, 1790–1801.

Felderhof, B.U., Ooms, G., 1989. Effective mass density of suspensions. Phys. Fluids A1, 1091–1097.

Felderhof, B.U., Ooms, G., 1990. Effect of inertia, friction and hydrodynamic interactions on turbulent diffusion. Eur. J. Mech. B/Fluids 9, 349–368.

Felderhof, B.U., Jansen, G.H., 1991. Linear dynamics of dilute hard-sphere suspensions. Physica A178, 444–466.

Gore, R.A., Crowe, C.T., 1989. Effect of particle size on modulating turbulent intensity. Int. J. Multiphase Flow 15, 279–285.

Hinze, J.O., 1975. Turbulence. McGraw-Hill, New York, p. 211.

Kenning, V.M., Crowe, C.T., 1997. On the effect of particles on carrier phase turbulence in gas–particle flows. Int. J. Multiphase Flow 23, 403–408.

Lun, C.K.K., Liu, H.S., 1997. Numerical simulation of dilute turbulent gas–solid flows in horizontal channels. Int. J. Multiphase Flow 23, 575–605.

Portela, L.M., Oliemans, R.V.A., Nieuwstadt, F.T.M., 1999. Numerical simulation of particle-laden channel flows with two-way coupling. In: Proc. 3rd. ASME/JSME Joint Fluids Engineering Conference, San Francisco, USA, July 18–23, 1–9.

Squires, K.D., Eaton, J.K., 1990. Particle response and turbulence modification in isotropic turbulence. Phys. Fluids 2, 1191–1203.

Yarin, L.P., Hetsroni, G., 1994. Turbulence intensity in dilute two-phase flow-3; the particles–turbulence interaction in dilute two-phase flow. Int. J. Multiphase Flow 20, 27–44.

Yuan, Z., Michaelides, E.E., 1992. Turbulence modulation in particulate flows — a theoretical approach. Int. J. Multiphase Flow 18, 779–785.